Applied Energy 374 (2024) 124000

Contents lists available at ScienceDirect

Applied Energy

journal homepage: www.elsevier.com/locate/apenergy

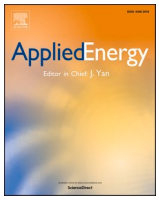

Assessing the feasibility of retrofitting parabolic trough power plants with integrated photovoltaic systems for grid integration

José A. López-Álvarez *, Miguel Larrañeta, Isidoro Lillo-Bravo, Manuel A. Silva-Pérez

Departamento de Ingeniería Energética, Universidad de Sevilla, Seville, Spain

HIGHLIGHTS

- Developed a dynamic open-source simulation tool for hybrid solar systems.
- Evaluated the optimal size of PV plant and electrical heater for retrofitting Parabolic Trough plants.
- Explored the incorporation of an electrical heater in Parabolic Trough TES systems.

ARTICLE INFO

Keywords:
Solar plants
Hybrid solar
Performance evaluation
Retrofitting

ABSTRACT

This study addresses the optimization issues of a Parabolic Trough (PT) power plant by retrofitting it with a photovoltaic (PV) plant to find the optimal configuration for already operational Concentrated Solar Power (CSP) plants. A simulation tool based on Modelica and OpenModelica has been developed to analyze and optimize the performance of CSP/PV hybrid plants under several grid limitation scenarios, one of which includes an electrical heater to utilize the PV surplus, considering the impact of hybridization on their overall performance and therefore also on their economic viability. The results obtained provide clear insights into how different configurations of CSP and PV plants interact and how certain variables, such as the PV ratio and thermal storage size, influence the overall performance of the hybrid plant.

1. Introduction

The transition of the energy system towards renewable energies is essential if we are to effectively address climate change and consolidate sustainable energy practices. According to the projections of the International Energy Agency's *Net Zero Emissions by 2050* scenario, an enormous increase in energy generation from renewable sources is expected globally, jumping from roughly 28% in 2021 to approximately 88% by 2050 [1]. According to the International Renewable Energy Agency (IRENA) [2], solar power increased by 650% in ten years, and it is expected to continue to develop at a rapid rate in the future.

CSP technology has proven its capacity to produce large-scale electricity, with 7 GW installed worldwide in 2021, and significant growth forecasts projecting 437 GW to be installed in 2050 in the Net Zero Emissions scenario. This forecast reflects the growing recognition of the benefits and potential of CSP technology in the development of renewable energies. CSP technology can store and supply electricity even after sunset and will play an essential role in the transition to more sustainable and emission-free energy systems. Despite this, there is still a way to go to achieve the success of PV plants, with 1046 GW installed worldwide as of 2023 [2]. One challenge of CSP technology is to reduce the high levelized cost of electricity (LCOE) compared to other forms of power generation, such as PV. The global weighted average LCOE for CSP stands at 0.118 USD/kWh, reflecting a reduction of 69% between 2010 and 2022. Meanwhile, the global weighted average LCOE for PV is 0.049 USD/kWh, indicating an 89% reduction over the same period [3].

The hybridization of CSP plants with PV presents itself as a solution to address the challenges faced by CSP (high cost of electricity) and PV (lack of economic and efficient solutions for large-scale electrical energy storage [4]) by combining the thermal storage capacity of CSP plants with the low-cost electricity production of PV plants. Hybridization allows increasing the penetration of solar power, reducing the impact on the power system. From the point of view of the CSP plants already in operation, the proposed hybridization helps reduce the LCOE [5–7], making these plants more attractive, competitive, and enhancing the profitability, operation, and performance of the operating CSP plants [8–11].

* Corresponding author at: Camino de los Descubrimientos s/n, 41092, Sevilla, Spain.
E-mail address: jlopez1@us.es (J.A. López-Álvarez).

https://doi.org/10.1016/j.apenergy.2024.124000
Received 22 April 2024; Received in revised form 28 June 2024; Accepted 21 July 2024
Available online 2 August 2024

Nomenclature

a	Empirical coefficient that establishes the upper limit for module temperature at low wind speeds and high solar irradiance
A_{mod}	Module Area
A_t	Total Annual Costs
b	Empirical coefficient that establishes the rate at which module temperature drops as wind speed increases
CF	Capacity Factor
$Cost_{EH}$	Total costs of the electrical heater updated to the reference year using the real interest rate
CSP	Concentrated Solar Power
CSP-ORC	Concentrated Solar Power - Organic Rankine Cycle
CPV	Concentrator Photovoltaic Cells
DC	Direct current
DNI	Direct Normal Irradiance
$E_{CSP_{AUX}}$	CSP parasitic
$E_{PV\ to\ CSP}$	PV energy used to satisfy the CSP parasitic
E_{CSP}	Energy yield of the standalone CSP plant
E_{PV}	Energy yield of the standalone PV plant
E_{total}	Energy yield of the hybrid plant
f_{PV}	Derating Factor
GHI	Global Horizontal Irradiance
GTI	Global Tilted Irradiance
GTER	Group of Thermodynamic and Renewable Energies - University of Seville
HCE	Heat Collecting Element
i	Real Interest Rate
I_O	Investment Costs
I_{ref}	Reference solar irradiance on module
LCOE	Levelized Cost of Electricity
$LCOE_{CSP}$	LCOE of the standalone CSP plant
$LCOE_{PV}$	LCOE of the standalone PV plant
$M_{t,el}$	Electricity production in the corresponding year
n	Economic Lifespan of the Plant
n_{mod}	Number of Modules
O&M	Operation and Maintenance
P_{CSP}	Nominal Power of the CSP Plant
P_{PV}	Nominal Power of the PV Plant
$P_{PV_{TOTAL}}$	PV Power Plant
P_{mod}	Module Power
PTC	Parabolic Trough Technology
PV	Photovoltaic
PV ratio	Ratio between the PV plant capacity and the CSP plant capacity
SAM	System Advisor Model
SM	Solar Multiple
SSR	Self-Supply Ratio
t	Corresponding Year. Year when the CSP plant is retrofitted with the PV plant, counted from the startup date of the CSP plant
T_{amb}	Ambient Temperature
T_c	Cell Temperature
$T_{c,ref}$	PV cell temperature under standard test conditions (25 °C)
T_m	Back-surface Module Temperature
TES	Thermal Energy Storage
TMY	Typical Meteorological Year
w_{sp}	Wind speed measured at standard 10-m height
y	Year when the retrofitting takes place
β	Tilt angle of the PV panel
γ	Surface Azimuth Angle
δ	Solar Declination
ΔT	Temperature difference between the cell and the module back surface at an irradiance level of 1000 W/m^2
η_{inv}	Inverter Efficiency
η_{PV}	Module Efficiency
$\eta_{PV,nom}$	Nominal Module Efficiency
θ	Incidence Angle
ρ	Albedo
τ	Temperature coefficient
ϕ	Latitude
ω	Hour Angle

Considering the remarkable benefits that hybridization brings, the retrofitting of operational CSP plants with PV emerges as an exciting solution. This approach offers accelerated implementation compared to the building of a new CSP/PV hybrid plant, because it capitalizes on the existing infrastructure of the CSP facility. By strategically integrating a PV plant into a CSP facility, we ensure optimal utilization of the solar resource available at the site, thus maximizing the electricity production potential.

The literature currently explores the retrofitting of CSP plants. Oyekale et al. [12] aim to investigate the techno-economic benefits of adapting biomass for existing CSP-ORC (Concentrated Solar Power - Organic Rankine Cycle) plants with Thermal Energy Storage (TES). The study is based on the existing CSP-ORC Fresnel plant in Ottana, Italy, with a power of 630 KW_e. The study proposes two biomass hybridization approaches: fixed (A biomass furnace is used to provide a constant supply of thermal energy to the ORC, ensuring a minimum electricity production) and modular (The biomass furnace is regulated to supply the thermal energy required to operate the ORC at its maximum capacity continuously). In addition to the biomass retrofit case study, they introduced a new integrated design case study, with modified solar field and TES capacity. The study demonstrates that the retrofit increases the annual net efficiency of the hybrid plant by 4–5 points compared to standalone CSP-ORC plants. It also shows that it can lead to an increase in full-load operating hours, where an implemented modular approach allows following a scheduled power profile, thereby enhancing dispatchability. Otanicar et al. [13] propose a retrofitting approach for CSP plants using a purely concentrator photovoltaic cell (CPV) design that integrates with the existing CSP plant architecture. The completed work represents a relatively simple way to preserve the existing infrastructure in the solar field while creating a means to generate electricity at low LCOE. This approach utilizes a Parabolic trough collector, a secondary concentrator, and CPV to achieve significant improvements in the efficiency and power of the CPV.

Goel et al. [14] study the hybridization of PTC plants with RP-3 mirrors without thermal energy storage by installing a dichroic mirror in the flow line between the primary mirror and the heat collecting elements (HCE), thereby reflecting part of the radiation spectrum to the PV receiver while transmitting the rest to the original HCE element in the existing PTC. Through this retrofitting of PTC plants, they achieve a 30% increase in annual production for plants with solar multiples (SM) greater than 1.5. Felsberge et al. [15] propose a new design and adaptation approach for a thermal system based on a PTC, where the absorber tube of a conventional PTC used in thermal systems is replaced with a hybrid absorber equipped with multi-junction solar cells, allowing for the retrofitting of existing CSP plants. In this study, the CSP plant produces district heating, and with the retrofitting, the PV plant can produce electricity complementarily. An electrical efficiency of 26.3% and a thermal efficiency of 48.8% are simultaneously achieved. Orosz et al. [16] study the hybridization of CSP plants using spectral radiation filters, with the adaptation of photons to the appropriate converter based on their wavelength. This system allows for the modernization of

standard commercial CSP plants, achieving production increases of approximately 10.7%.

Carvajal et al. [17] present a preliminary technical and economic analysis of integrating a PV plant into a PTC plant to reduce electricity generation costs. An integrated CSP/PV model is used for simulations, assessing different PV plant sizes and auxiliary consumption scenarios. The results reveal that the optimal PV plant capacity depends on the auxiliary consumption of the PTC plant and that PV integration improves the LCOE in all cases. The importance of analyzing both plants in an integrated manner is emphasized to achieve greater efficiency and cost reduction. Similarly, Bode et al. [18] analyze the integration of CSP plants with PV energy to enhance efficiency and profitability. Their study emphasizes the retrofitting of existing CSP plants with PV to reduce auxiliary load and increase electricity production. They present a simulation model and a case study in South Africa, where they conclude that CSP/PV retrofitting can significantly improve the profitability of existing CSP plants, with an optimal PV installation size of approximately 7 MWAC for 50 MW CSP plants.

Riffelmann et al. [19] study various CSP/PV hybridization options, including covering the self-consumption of the CSP plant directly with a PV plant. To do this, they select the size of the PV plant based on the maximum parasitic load of the CSP plant, obtaining promising results in terms of LCOE reduction due to the lower price of PV electricity during daylight hours.

This study addresses the optimization issues of a CSP plant through retrofitting with a PV plant, aiming to find the optimal configuration for an already constructed CSP plant. The focus lies in increasing the capacity of the PV plant to meet the self-consumption requirements of the CSP plant and enhance the hybrid plant's production in various scenarios, which will be described later. In addition, we present an economic analysis to select the optimal plant size. To utilize surplus PV energy that cannot be injected into the grid or allocated for the CSP plant's self-consumption, we implement an electrical heater in the model in parallel to the CSP field. This enables the heating of molten salts with the electricity generated by the PV field. The use of electric heaters in hybrid plants is a concept currently under study. Gedle et al. [20] study the diversion of surpluses from PV plants to electric heaters in a hybrid plant to increase the temperature of salts and thus improving the performance of the TES compared to co-located hybrid plants. The results show LCOE reductions of up to 20% compared to co-located plants. Pilotti et al. [21] state that the implementation of electric heaters results in an LCOE reduction ranging from 3.6% to 10%, depending on the plant's operational strategy. Richter et al. [22] demonstrate a predictive control strategy in hybrid plants with electric heaters, showing that this strategy provides better results compared to a heuristic approach. It improves performance and optimizes the plant configuration.

The substantial innovation of this study lies in the exploration of the optimal configuration (size and tilt) for PV plants in the retrofitting of existing CSP facilities with the aim of reducing the self-consumption of these plants and supplying that energy with PV, thereby producing cheaper electricity and increasing the capacity of the CSP plant to feed into the grid by reducing the amount of energy used to cover its self-consumption. This is done by considering various realistic grid limitation scenarios through a detailed sensitivity analysis of the critical parameters affecting these plants, as well as the use of Pareto frontiers with the aim of establishing optimal configurations for scenarios requiring multi-objective optimization. The study examines the energy and economic impact by calculating the LCOE of the retrofitted plant, also considering the timing of the retrofitting. To this end, an open-source tool is introduced, enabling the smooth integration of both technologies. Specific parameters crucial for evaluating this adaptation are explained, such as the Self-Supply Ratio (SSR), which quantifies the percentage of self-consumption supported by PV energy. Additionally, the study strategically addresses the potential incorporation of electric heaters in the modernization of these plants, aiming to enhance their competitiveness and economic efficiency by capitalizing on the surpluses generated by PV energy. To determine the impact of the costs associated with this type of plant in these studies, we will conduct an economic analysis considering different future price scenarios. This analysis will allow us to evaluate how energy generation costs vary based on projected changes in the prices of the main components in the retrofitting of these plants.

This paper is organized as follows: Section 2 presents the performance tool to simulate hybrid PV/CSP plants. Section 3 outlines the configurations and the indicators used to evaluate the performance of the different CSP plants and scenarios. Results and discussions of the simulation are provided in Section 4. Finally, Section 5 presents a summary of this study and provides the main conclusions.

2. Performance tool

A detailed simulation of a hybrid power plant combining PV and CSP technologies is necessary to understand its performance and evaluate its sustainability in production. In this context, ASDELSOL, a simulation tool developed in Modelica [23] using OpenModelica [24], facilitates the analysis and optimization of PV-CSP generation systems.

We developed a Modelica library specifically designed to assess solar resources and perform solar calculations. This library plays a fundamental role in determining the behavior of hybrid power plants.

2.1. Solar resource

The Solar Resource library takes a Typical Meteorological Year [25] and the geographic coordinates of the selected location as input. Using this information, the library allows for the determination of the sun's position at all times, as well as the Global Tilted Irradiance (*GTI*) [26], which is an essential parameter for analyzing PV plants, using (1).

$$GTI = DNI \cdot cos(\theta) + DHI \cdot \frac{1 + cos(\theta)}{2} + GHI \cdot \rho \cdot \frac{1 - cos(\theta)}{2} \quad (1)$$

where *DNI* is the Direct Normal Irradiance, θ is the incidence angle [27], *DHI* is the Diffuse Horizontal Irradiance, *GHI* is the Global Horizontal Irradiance, and ρ is the albedo. To calculate θ, we use (2).

$$\begin{aligned}\theta = \text{acos}[&sin(\delta)\cdot sin(\phi)*cos(\beta) - sin(\delta)\cdot cos(\phi)*sin(\beta)\cdot cos(\gamma)\\ &+ cos(\delta)\cdot cos(\phi)\cdot cos(\beta)\cdot cos(\omega) + cos(\delta)\cdot sin(\phi)\cdot sin(\beta)\cdot cos(\gamma)\cdot cos(\omega)\\ &+ cos(\delta)\cdot sin(\beta)\cdot sin(\gamma)\cdot sin(\omega)\,]\end{aligned} \quad (2)$$

where δ is the solar declination, ϕ is the latitude, β is the tilt angle of the PV panel, γ is the surface azimuth angle and ω is the hour angle.

2.2. CSP system

This simulation tool incorporates a specific library to simulate the Parabolic Trough Technology (PTC), extending the existing capabilities of the Solartherm library [28] which is focused on the central receiver tower technology. The new CSP library is designed to provide accurate models of PTC power plants. We have chosen this type of CSP plant because, focusing on the modernization of CSP facilities, most operational plants in Spain use this technology (45 out of 49 plants in operation [29]). These collectors are modeled based on specific parameters and characteristics obtained from the System Advisor Model (SAM) database [30] or from manufacturers' specifications. A crucial aspect in accurately capturing the performance of the collectors is the calculation of the collectors' optical performance. To address this, the CSP library incorporates an optical efficiency matrix that accounts for the solar position of the detailed collectors [31]. This matrix illustrates the optical performance of the PTC, representing the ratio between power in the receiver and power in the aperture area for each sun position based on azimuth and zenith angle. This matrix only captures optical losses; the thermal losses from the field are modeled in ASDELSOL. The calculation

Table 1
Main characteristics of EuroTrough PTC.

Parameter	Value
Reflective aperture area (m^2)	817.5
Aperture width total structure (m)	5.77
Length of collector assembly (m)	148.5
Number f modules per assembly	12
Focus Length (m)	1.71

of this optical efficiency matrix should be done using external software tools, such as Tonatiuh [32] or SolTRACE [33]. In the study, we simulate a loop of PTC EuroTrough [34] (Table 1) in Tonatiuh to calculate the optical efficiency matrix, and we use the same PTC in the different configurations of the hybrid plants.

2.3. PV system

PV model is a mathematical framework developed to provide a realistic estimation of energy production in PV systems. Simulated PV plants are considered to have fixed panel inclinations. To account for the environmental factors associated with the specific location, the calculation of the cell temperature (T_c) [35] is performed as a primary step combining (3) and (4). Subsequently, the module efficiency is determined, enabling the calculation of the power output [36] using (5) and (6) respectively.

$$T_m = T_{amb}^2 + GTI \cdot e^{a+b \cdot w_{sp}} \tag{3}$$

where T_m is the back-surface module temperature, a is the empirical coefficient that establishes the upper limit for module temperature at low wind speeds and high solar irradiance, b is the empirical coefficient that establishes the rate at which module temperature drops as wind speed increases, w_{sp} is the wind speed measured at standard 10-m height and T_{amb} is the ambient temperature.

$$T_c = T_m + \frac{GTI}{I_{ref}} \cdot \Delta T \tag{4}$$

where T_c is the cell temperature, I_{ref} is the reference solar irradiance on module and ΔT is the temperature difference between the cell and the module back surface at an irradiance level of 1000 W/m^2.

$$\eta_{PV} = \eta_{PV,nom} \cdot \left[1 + \tau \cdot \left(T_c - T_{c,ref}\right)\right] \tag{5}$$

where η_{PV} is the module efficiency, $\eta_{PV,nom}$ is the nominal module efficiency, τ is the temperature coefficient and $T_{c,ref}$ is the PV cell temperature under standard test conditions (25 °C).

$$P_{mod} = \mathrm{A_{mod}} \cdot \eta_{PV} \cdot \eta_{inv} \cdot f_{PV} \cdot GTI \tag{6}$$

where P_{mod} is the module power, $\mathrm{A_{mod}}$ is the module area, η_{inv} is the inverter efficiency and f_{PV} is the derating factor, which accounts for the soiling of the panel, loss in wirings, shading and other secondary losses. The PV power plant production ($P_{PV_{TOTAL}}$) can be calculated with (7), where $\mathrm{n_{mod}}$ is the number of modules.

$$P_{PV_{TOTAL}} = \mathrm{P_{mod}} \cdot \mathrm{n_{mod}} \tag{7}$$

2.4. Validation

To validate ASDELSOL, results from CSP and PV plant simulations are compared with SAM. For the CSP plant, the Andasol I [37] plant has been modeled in both software with a TMY data from Sevilla. The annual net production results obtained through SAM amounted to 130.35 GWh, whereas ASDELSOL yielded annual net production results of 132.13 GWh. The difference between the two software tools is 1.36%. We compare the productions of the TES 4 h and TES 15 h configurations as well, obtaining differences of 2.11% and 1.79%, respectively. Regarding the PV plant, a 60 MW direct current (DC) plant has been modeled in ASDELSOL and SAM with a DC/AC ratio of 1.2, a $\eta_{PV,nom}$ of 19%, a $\mathrm{A_{mod}}$ of 1.63 m^2, a inverter efficiency (η_{inv}) of 96% and a derating factor (f_{PV}) of 14%, and the production in annual net production in SAM results in 92.72 GWh, while in ASDELSOL it is 92.50 GWh. The difference between SAM and ASDELSOL is 0.24%. Fig. 1 shows the power output of the PV and CSP plants over three days in SAM and ASDELSOL. The PV power output is nearly identical between both tools, while the CSP power output shows more significant differences. This is because ASDELSOL models the start-up cycle of the power cycle with a "start-up" state where the turbine requires time to warm up before producing power, ramping up in steps until reaching nominal power (resulting in minor differences during start-up). Additionally, ASDELSOL controls the TES discharge pump and the solar field pump to maintain the turbine's nominal power as constant as possible, leading to differences between SAM and ASDELSOL during TES engagement. Consequently, the available energy in the TES in ASDELSOL is used to avoid the drop observed in SAM, resulting in slightly less energy at the end of the day.

2.5. Economic assessment

The economic assessment plays a fundamental role in the feasibility of solar power plants. In this study, our focus is on calculating the LCOE for a CSP/PV hybrid plant, considering the impact of hybridization on its overall performance and therefore also on its economic viability.

A critical aspect to consider during the retrofitting process of CSP plants is determining the optimal timing for such action within the plant's lifespan.

The LCOE of the standalone CSP plant must be estimated first to calculate the LCOE of the hybrid plant. We differentiate between two types of auxiliary consumption in the CSP plant, online and offline [38]. Online auxiliary consumption refers to those that can be covered by the plant itself, either by the turbine or by the PV plant when hybridization exists, while offline auxiliary consumption refers to those that cannot be covered by the plant and must be purchased from the grid, imposing a purchase price for that energy (PPA) with a fixed value of 0.12 €/kWh.

For calculating the LCOE of CSP and PV plants independently, we use (3) [39]:

$$LCOE = \frac{I_O + \sum_{t=1}^{n} \frac{A_t}{(1+i)^t} + \sum_{t=1}^{n} \frac{E_{grid} \cdot PPA}{(1+i)^t}}{\sum_{t=1}^{n} \frac{M_{t,el}}{(1+i)^t}} \tag{3}$$

where I_O is the investment cost, A_t are total annual costs without taking into account the costs of purchasing electricity from the grid to cover offline auxiliary consumption, E_{grid} are the offline auxiliary consumption, $M_{t,el}$ is the electricity production in the analyzed year, i is the real interest rate, n is the economic lifespan of the plant and t is the corresponding year.

To calculate the LCOE of the hybrid CSP/PV plant we use (4), considering that for the PV plant and the electrical heater, it is computed from the year of its installation until the end of the operational life of the CSP plant:

$$LCOE_{Hybrid} = \frac{y \cdot (LCOE_{CSP} \cdot E_{CSP}) + (n-y) \cdot (LCOE_{PV} \cdot E_{PV} + LCOE_{CSP} \cdot E_{CSP} + Cost_{EH})}{(n-y) \cdot E_{total} + y \cdot E_{CSP}} \tag{4}$$

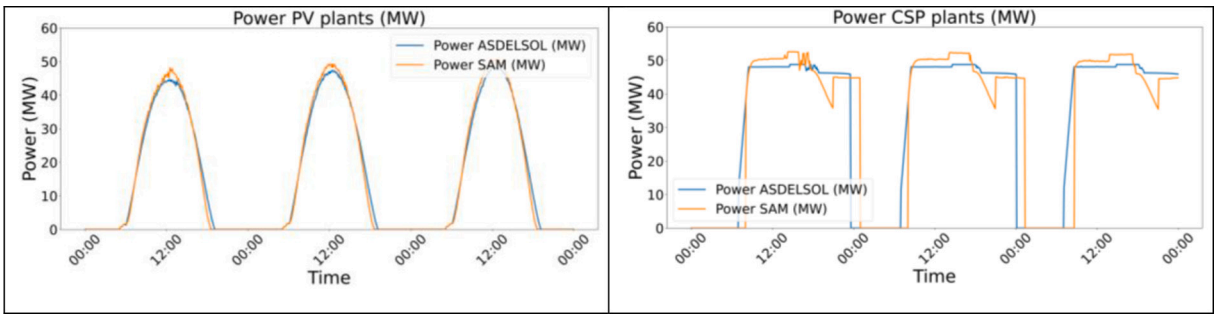

Fig. 1. Comparison of PV and CSP Plants in ASDELSOL and SAM.

where y denotes the year when the retrofitting takes place (In all the cases studied, we consider that the retrofitting takes place at the midpoint of the CSP plant's lifespan), $LCOE_{CSP}$ is the standalone CSP plant's cost of energy, E_{CSP} denotes it's production, $LCOE_{PV}$ is the standalone PV plant's cost of energy, E_{PV} is the increase in production brought on by the retrofitting relative to the standalone CSP plant, $Cost_{EH}$ are the total costs of the electrical heater, if it's applicable, updated to the reference year using the real interest rate and E_{total} is the hybrid plant's production.

Table 2. Economic data.

The economic analysis of hybrid CSP/PV plants is crucial for evaluating their performance and viability. The influence of costs is especially relevant, so we have considered three future price scenarios for PV technology (which has been used in the retrofitting of operational CSP plants) according to the projections of the National Renewable Laboratory Annual Technology Baseline (NREL ATB) [40]. The scenarios are detailed in the Table 3.

3. Performance assessment

3.1. CSP plant configuration

In this section, we present the different configurations of CSP plants subject to retrofitting. We choose the Andasol I plant configuration, with a nominal capacity of 50 MW and a storage of 7.5 h, as the base case [37]. Subsequently, the same plant configuration will be analyzed but with different storage hours. This analysis will involve optimizing the SM for each configuration and, consequently, adjusting the size of the solar field to observe the effect of retrofitting in these new configurations. We select Seville as the location for the plants, using a TMY elaborated by GTER as the solar resource input. Due to the optimal balance between the calculation time and the accuracy of the results [43], the simulation is performed with a 5-min time resolution. Table 4 summarizes the main characteristics of the analyzed CSP plants.

Table 2
includes the main proposals and economic data considered for the economic analysis of the hybrid plant retrofitting process.

Parameter	Value	Unit
PV plant [40]		
CAPEX	1.20	€/W_p
O&M	20.95	€/KW_p-yr
CSP plant [41]		
Solar field	132	€/m^2
HTF system	52.80	€/m^2
TES system	54.56	€/kWh_t
Power block	800.8	€/kW
Auxiliary system	79.20	€/kW
O&M	60.06	€/kW-yr
Electrical heater [42]		
General cost	0.08	€/W

Table 3
Economic data for three different scenarios.

		2021	2030	2050
Conservative	CAPEX (€/Wp)	1.20	1.12	0.77
	O&M (€/kWp)	20.95	18.54	14.68
Moderate	CAPEX (€/Wp)	1.20	0.96	0.58
	O&M (€/kWp)	20.95	16.72	12.55
Advanced	CAPEX (€/Wp)	1.20	0.85	0.48
	O&M (€/kWp)	20.95	15.32	10.85

Table 4
Main characteristics of the analyzed CSP plants.

Power Plant	Nominal Turbine Capacity (MW)	Storage Capacity (hours)	SM	Annual Production (GWh)	LCOE (€/kWh)
Andasol I	50	4	1.5	89.5	0.216
Andasol I	50	7.5	2.23	132.13	0.20
Andasol I	50	15	2.75	164.57	0.217

3.2. Grid limitation scenarios

After retrofitting, hybrid plants use a variety of operational scenarios depending on their capacity to feed excess photovoltaic (PV) energy into the grid. The primary goal of the PV plant in any scenario is to meet the auxiliary consumption of the CSP plant (self-consumption). In the first scenario (a), hybrid plants are allowed to inject any extra PV production not used for the CSP plant's self-consumption into the grid. In the second scenario (b), the hybrid plant can supply a maximum power corresponding to the nominal power of the CSP plant. Any additional surplus energy from the PV plant beyond this capacity cannot be injected into the grid. In the third scenario (c), only the CSP plant is allowed to supply energy to the grid, and the PV plant can only be used to cover the hybrid plant's own consumption.

We consider a new scenario (d), which is similar to scenario (b), with the only difference being that we introduce electrical heaters to harness the surplus PV energy to heat molten salts. This increases the charging capacity of the TES thanks to this extra energy. In all configurations, the energy for the CSP plant's self-consumption that cannot be covered by

Table 5
Characteristics of the proposed scenarios for hybrid plants.

Scenario	Feed to grid from PV	PV Excess	Electrical Heater
a	Yes	No	No
b	Yes (up to CSP power)	Yes	No
c	No	Yes	No
d	Yes (up to CSP power)	Yes	Yes

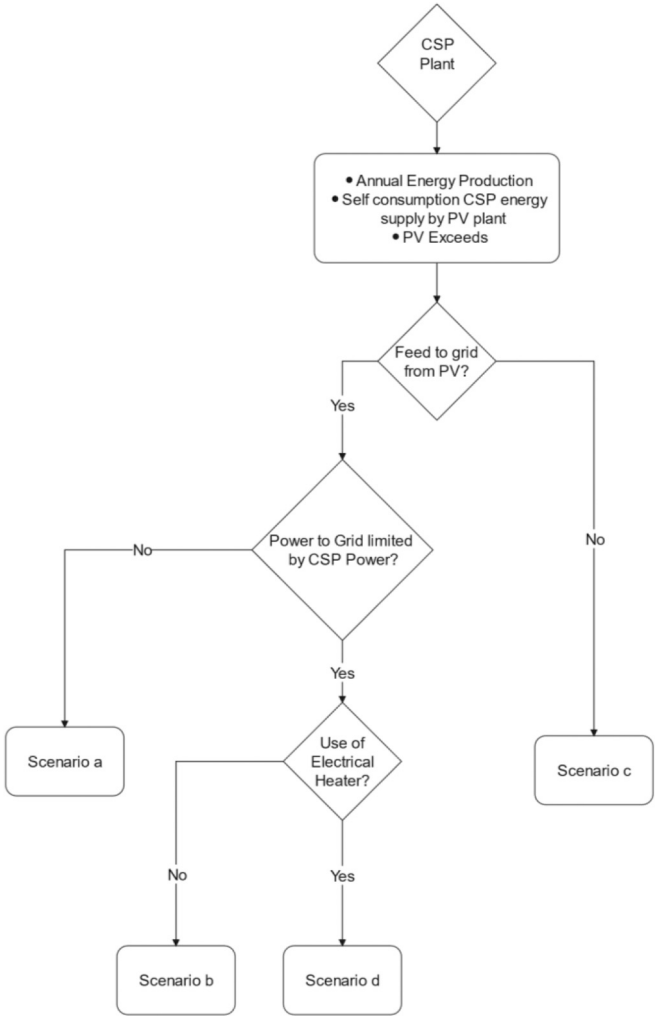

Fig. 2. Flowchart of the methodology.

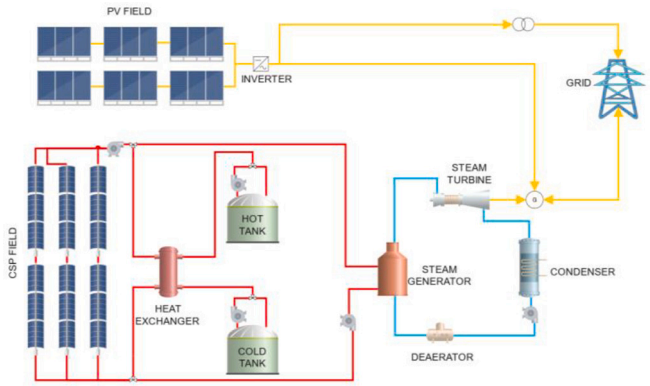

Fig. 3. Hybrid CSP/PV plant layout for scenarios (a) and (b).

either the PV plant or the CSP plant (E_{grid}) is supplied from the electric grid, purchased at the PPA price. Table 5 shows the 4 proposed scenarios and their respective characteristics, while Fig. 2 summarizes the methodology to determine the analyzed scenario based on whether the PV plant can feed energy into the grid or not, or if, in the case that it can feed into the grid, there is a power limitation at the connection point (in addition to whether we consider electrical heaters or not).

The configuration of the plants is the same in scenarios (a) and (b) as we can see in Fig. 3, but they differ mainly in the capacity to feed energy

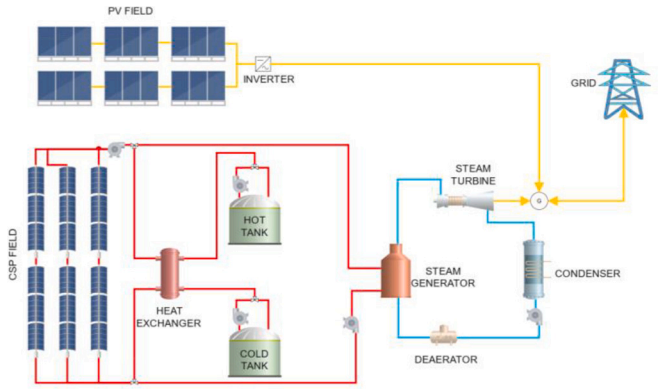

Fig. 4. Hybrid CSP/PV plant layout for scenarios (c).

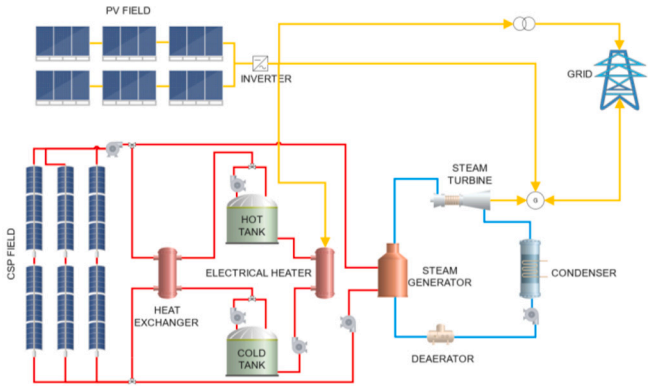

Fig. 5. Hybrid CSP/PV plant layout for scenarios (d).

into the grid from the PV plant. The energy flows from the PV and CSP plants are represented by arrows. Fig. 4 shows the configuration of scenario (c), where the energy from the PV plant is only used to cover the self-consumption of the CSP plant. Fig. 5 shows the plant configuration for the scenario (d), which includes the integration of electric heaters that use surplus PV energy that cannot be directly fed into the grid, because plant capacity is exceeded.

3.3. Metrics

A set of indicators are defined to help in the assessment of the performance, efficiency and viability of hybrid plants and the effect of retrofitting.

The economic viability of CSP/PV hybrid plants is evaluated using the LCOE, as described above. The LCOE provides a measure of the average cost of electricity generated by the plant over its lifetime, considering investment costs, operational costs, and the generated energy.

To assess the performance of the hybrid plant, we use the Capacity Factor (CF) and the SSR.

The CF is a measure of the energy production generated by a plant relative to its maximum output (Operating at its nominal power for all 8760 h of the year). In the hybrid plant, we define the CF depending on the maximum power that the plant can inject into the grid. In the case of scenario (a), we use eq. (Eq. (10)), while for the rest of the scenarios, where the maximum power that can be fed into the grid is limited by the nominal power of the CSP plant, we use eq. (11).

$$CF = \frac{E_{total}}{(P_{CSP} + P_{PV})*8760\ h/year} \tag{10}$$

$$CF = \frac{E_{total}}{P_{CSP}*8760\ h/year} \tag{11}$$

where E_{total} is the production of the hybrid plant, P_{CSP} is the gross nominal power of the CSP plant and P_{PV} is the DC power of the PV plant.

The SSR is an indicator that shows the proportion of energy demand from the CSP plant that can be met with internally generated PV energy. We calculate this parameter according to (12).

$$SSR = \frac{E_{PV\ to\ CSP}}{E_{CSP_{AUX}}} \tag{12}$$

where $E_{PV\ to\ CSP}$ is the PV energy used to satisfy the CSP auxiliary energy and $E_{CSP_{AUX}}$ is the CSP auxiliary energy (online and offline auxiliary consumption).

The ASDELSOL tool provides comprehensive annual information for hybrid plants, including both energy metrics (annual production, CF or SSR, for example) and economic metrics (LCOE). For multi-objective optimization processes, such as increasing CF while reducing LCOE, the tool includes calculations of Pareto frontiers for various plant configurations, when the users can pre-select the variables to be optimized. Fig. 6 illustrates the simulation and optimization process using the ASDELSOL tool.

4. Results and discussion

To conduct the optimization of the hybrid plant, a sensitivity analysis will be performed, considering parameters such as the size of the PV plant with the PV ratio (ratio between the PV plant capacity and the CSP plant capacity), the inclination of the PV panels, and, if applicable, the electrical heater's size (electrical heater size relative to PV field). The variables for the parametric analysis are detailed in the Table 6.

4.1. No PV discharge limitation. Scenario (a)

In Fig. 7, Fig. 8 and Fig. 9, we can observe the CF, LCOE, and SSR for the three analyzed CSP plant configurations with PV tilt 0°, 25°, and 35°. In a scenario where all excess PV energy can be fed into the grid, it is evident that as the PV ratio increases, the CF decreases, regardless of the storage capacity. This decline becomes more significant as storage capacity increases.

The influence of TES hours is related to the production capacity in the three configurations. In the case of three plants with the same nominal power, the plant with the largest storage capacity can generate a larger amount of energy. Therefore, when hybridized with PV, plants with higher storage capacity experience a more aggressive decline in their CF, compared to plants with lower storage capacity, with respect to their configuration as CSP-only plants.

Table 6
Variables in the sensitivity analysis.

Variable	Range	Step
PV ratio (%)	[0–200]	10
PV tilt (°)	[0–40]	5
Electrical heater size (%)	[20–100]	20

The LCOE reduction achieved with the retrofitting is, in this case, greater for the plants with smaller TES capacity. For example, the LCOE for a plant with 4 h TES goes from 0.216 €/kWh for a CSP-only plant to 0.1323 €/kWh for a hybrid plant with a 200% PV ratio and a PV tilt of 25° (38.7% reduction), while for a 15 h TES plant, the reduction is only from 0.217 €/kWh to 0.1537 €/kWh from the same configuration (29.2% reduction).

If we observe the SSR, we can notice that in the three analyzed configurations, there is a point of the PV ratio (approximately 50%) from which the effect is very low, until it becomes practically constant.

It is also observed that as the TES capacity increases for the same PV ratio, the SSR decreases. This is because with more hours of storage, the CSP plant can operate for longer periods during the night. The nighttime consumptions cannot be covered with the PV production.

Fig. 10 shows the annual distribution of auxiliary consumption of the CSP plant and the SSR for a specific case with a PV ratio of 100% and a panel tilt angle of 25° (the optimum tilt in this case). This representative example illustrates a trend observed in all configurations, as depicted in Fig. 9. The auxiliary energy consumption of the CSP plant has been normalized for each hour of the year, dividing the energy consumed in each hour by the total annual consumption. This analysis provides a picture of the temporal distribution of self-consumption in the CSP plant for different TES capacities. During sunlight hours, between 8:00 and 16:00, the SSR reaches 100% in all three configurations, indicating complete self-consumption during these periods. However, outside of this interval, the SSR starts to decrease and is null during night hours.

The distribution of energy among the three configurations shows that the plant with a 4 h TES system concentrates most self-consumption during sunlight hours due to its limited storage capacity. As the TES capacity increases, nighttime consumption increases and the relative

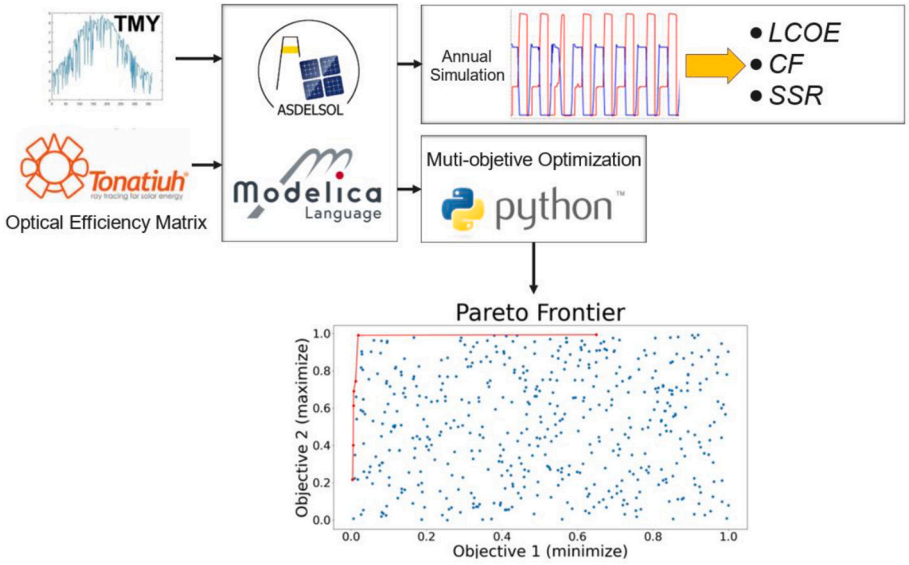

Fig. 6. Flowchart of ASDELSOL tool.

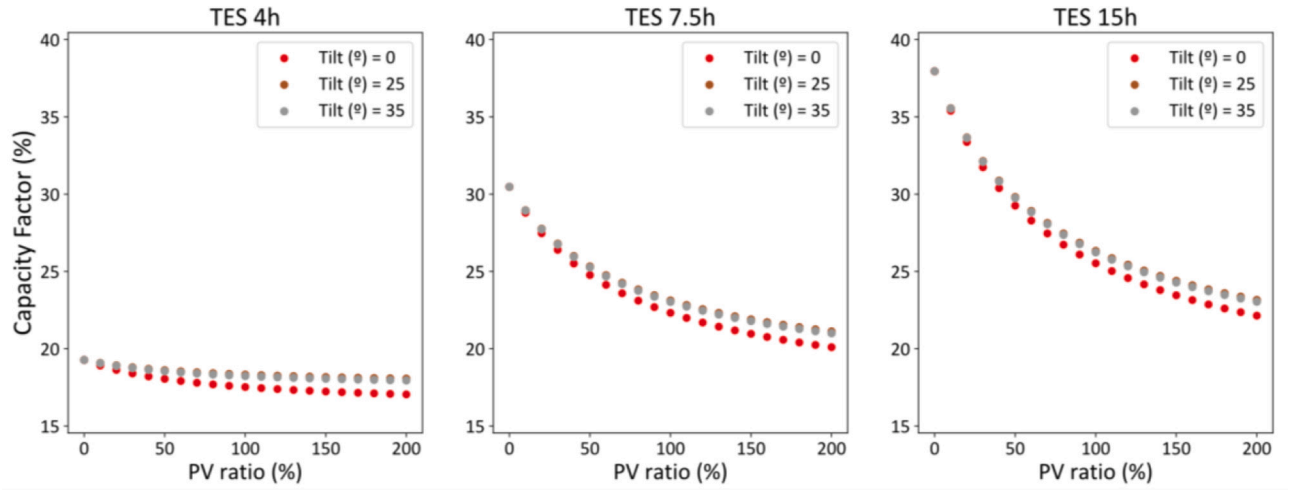

Fig. 7. Capacity Factor for the different hybrid CSP/PV configurations in scenario (a).

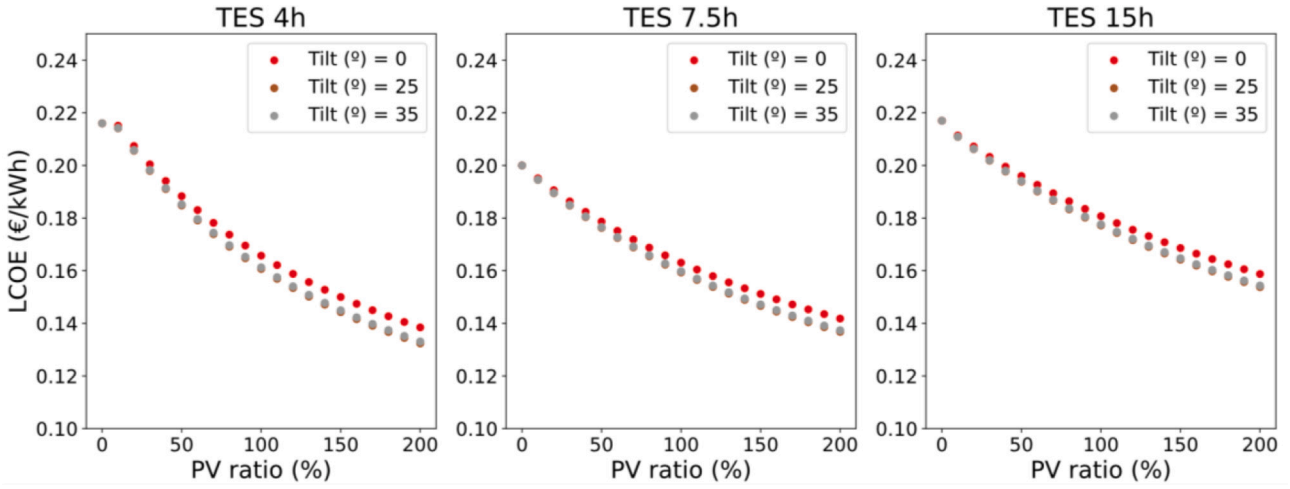

Fig. 8. LCOE for the different hybrid CSP/PV configurations in scenario (a).

weight of daytime consumption decreases. Combining both factors, concentrating energy self-consumption during hours with higher SSR increases the plant's annual SSR, as observed in the 4-h TES configuration. Conversely, if the CSP plant self-consumption is more evenly spread in time, the annual SSR decreases.

To determine the optimal configuration for each plant, we are calculating the Pareto frontiers between CF and LCOE (Fig. 11) and SSR and LCOE (Fig. 12). The Pareto frontier, a concept originating from

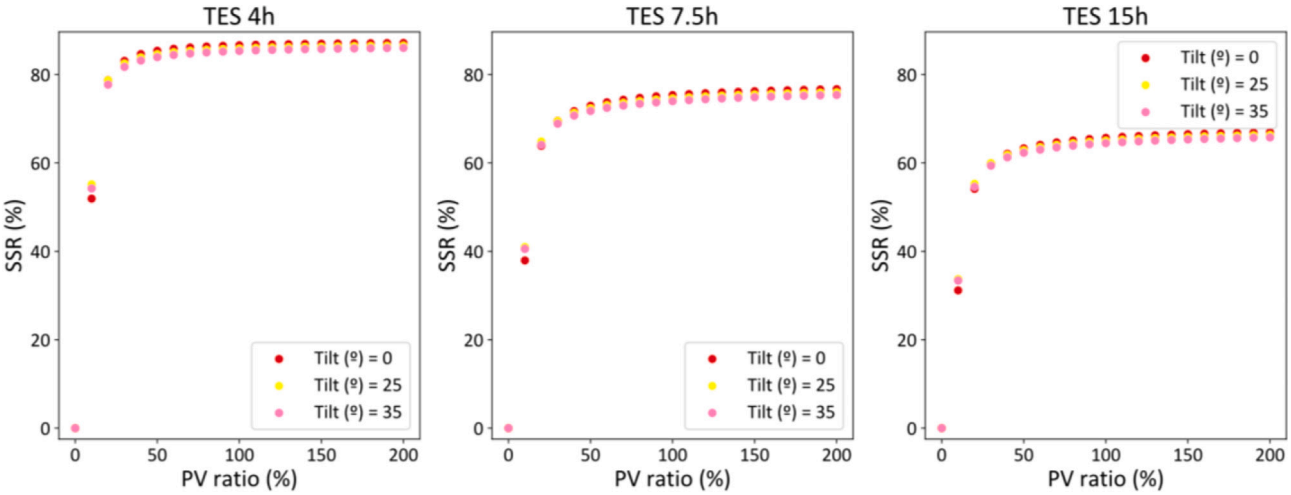

Fig. 9. Self-Supply Ratio for the different hybrid CSP/PV configurations in scenario (a).

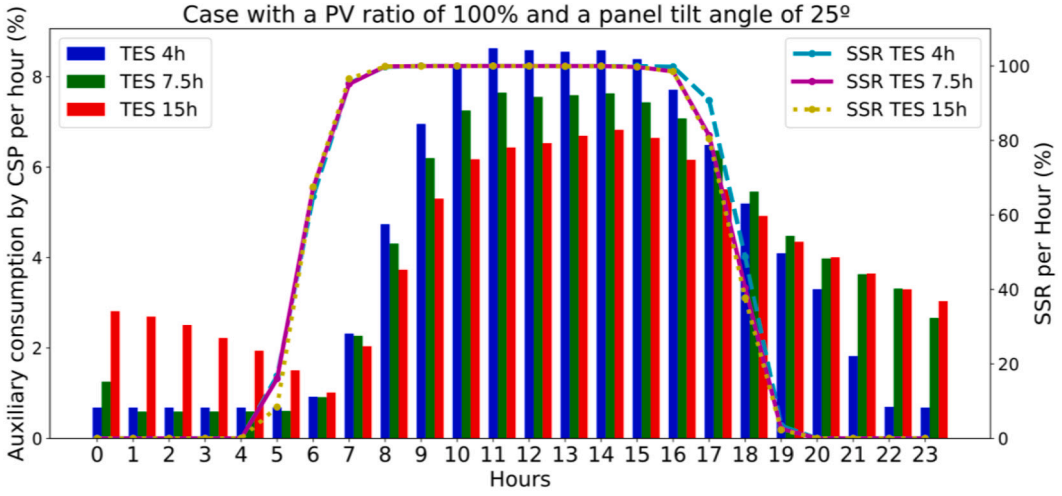

Fig. 10. Annual Distribution of auxiliary consumption from CSP and SSR for a hybrid plant with PV ratio = 100%.

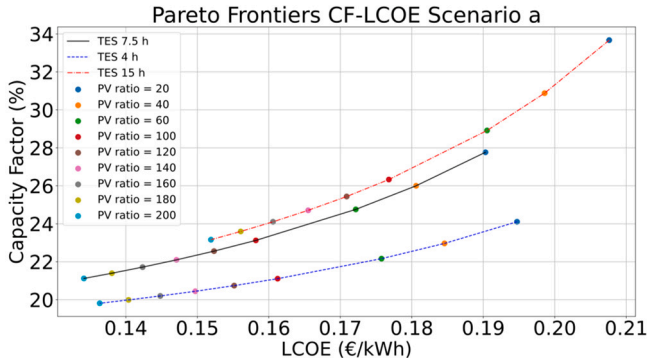

Fig. 11. Pareto Frontiers CF-LCOE scenario (a).

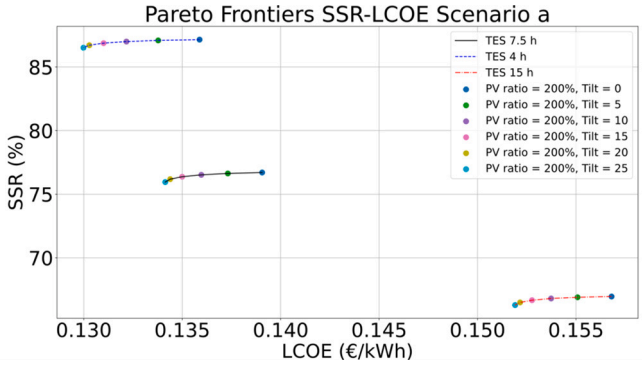

Fig. 12. Pareto Frontiers SSR-LCOE scenario (a).

multi-objective optimization, represents the trade-offs between conflicting objectives, aiming to maximize one without sacrificing the other. For the three plants under study, we find that the Pareto frontier between CF and LCOE is formed by points corresponding to a PV tilt of 25°. This specific tilt angle is identified as maximizing annual PV production. Furthermore, given that all PV energy can be efficiently integrated into the grid in this scenario, the optimal CF configuration is achieved at these values. In terms of SSR, the optimal configuration for all plants is attained with a PV ratio of 200% and a tilt ranging from 0° to 25°. This preference is attributed to the ability to satisfy higher levels of self-consumption with increasing PV ratio. Additionally, since all surplus PV energy can be seamlessly exported to the grid, enlarging the PV plant size does not adversely affect the LCOE.

In the Fig. 11, it can be observed that for the same PV ratio level (200%), the 15 h TES achieves a higher capacity factor (CF) due to nighttime generation, compared to the 4 h and 7.5 h TES configurations. However, this results in lower solar share ratio (SSR) for these configurations, as the nighttime generation cannot be covered by PV, as shown in the Fig. 12.

4.2. PV discharge limited to CSP nominal power. Scenarios (b) and (d)

In scenario (b), it can be observed that in the 3 analyzed configurations of Fig. 13, as the PV ratio increases the CF increases rapidly up to PV ratios of 20%, and then continues to rise, albeit with a smoother growth.

This is because the PV plant's ability to inject a certain quantity of electricity into the grid is constrained. A certain quantity of PV energy cannot be used when we increase the PV ratio, which penalizes the CF. Even if the PV plant's size has grown, not all the energy generated can be used to its full potential.

Regarding the LCOE, as shown in Fig. 14, the three configurations show that a minimum is reached for a specified PV ratio (130% for 4 h TES with tilt 25°, 80% for 7.5 h TES with tilt 25° and 90% for 15 h TES with tilt 25°). From these points, growing the PV plant's size starts to have less effect on the hybrid plant's overall output. With a limitation on grid injection for the hybrid plant, where the limitation lies in the PV plant, it makes sense that as the impact of As the PV on the total energy injected into the grid increases, the optimal size of the PV plant is found in larger plants. This occurs with low storage sizes, which inject less energy into the grid than plants with large storage capacities, allowing more room for injection by the PV plants. Therefore, as the size of the TES increases, the optimum is reached at lower PV ratios. The change in trend in the TES 15 h configuration is because, with large storage capacities, offline auxiliary consumption decrease as the plant operates more hours throughout the year. This reduces the need to purchase energy from the grid, impacting the LCOE by reducing expenses. Consequently, it becomes possible to increase the size of the PV plant without such a drastic impact on the LCOE, while also increasing the injection of PV energy into the grid.

The SSR maintains the same behavior as in scenario (a), reaching a constant value again from a PV ratio around 50%, as can be observed in Fig. 15.

Once the configurations for scenario (b) have been examined, we analyze the possibility of utilizing the unused PV energy to produce heat by introducing an electrical heater (scenario (d)). In this scenario, we have a new variable to analyze besides the PV ratio and tilt: the electrical

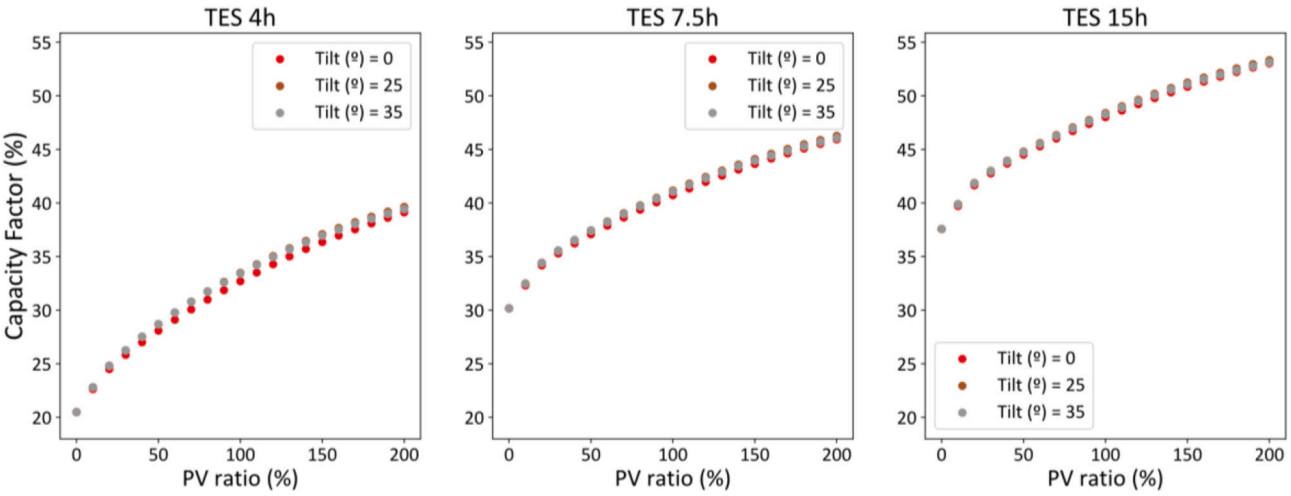

Fig. 13. Capacity Factor for the different hybrid CSP/PV configurations in scenario (b).

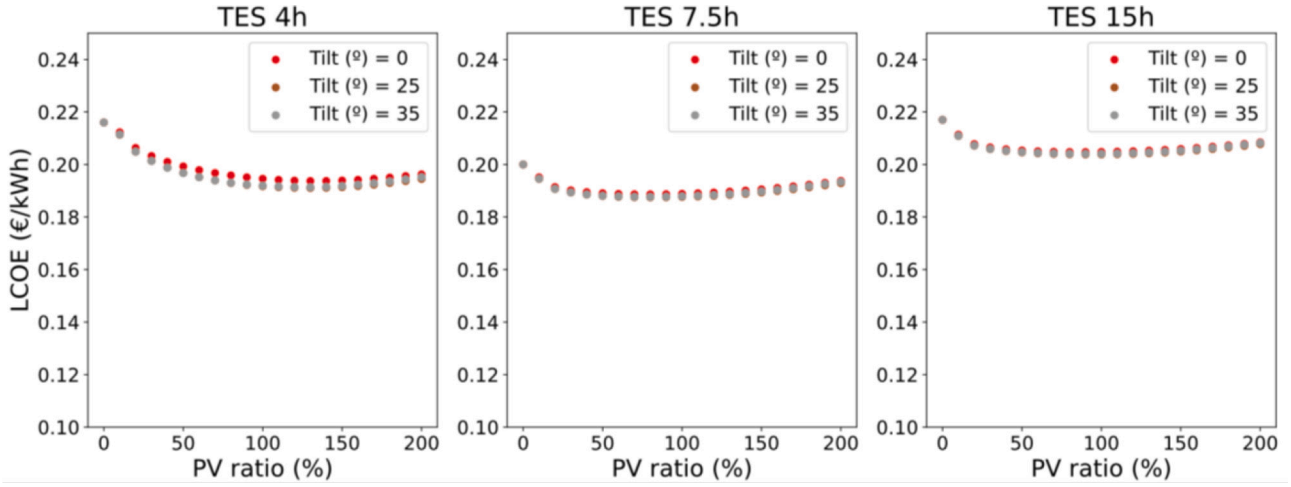

Fig. 14. LCOE for the different hybrid CSP/PV configurations in scenario (b).

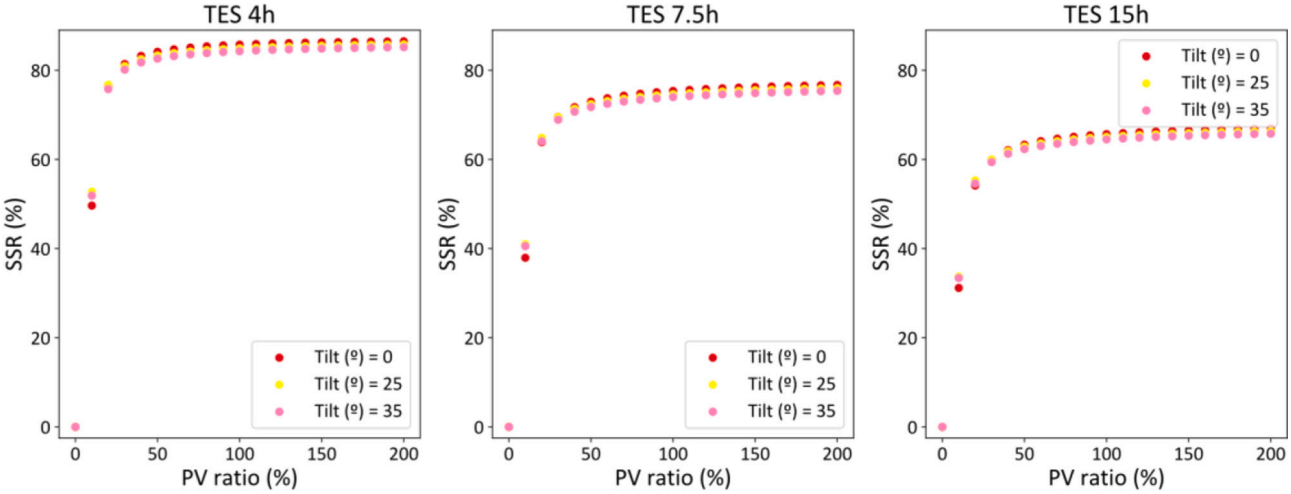

Fig. 15. Self-Supply Ratio for the different hybrid CSP/PV configurations in scenario (b).

heater's size. To achieve a more comprehensive understanding of the influence of various parameters on plant behavior and outcomes, heatmaps illustrating the correlation between electrical heater size and the PV ratio, along with the optimal tilt inclination of the PV panel in this scenario, are presented in Fig. 16, Fig. 17 and Fig. 18. In Fig. 16, we can observe the evolution of the CF in this scenario, which follows the same

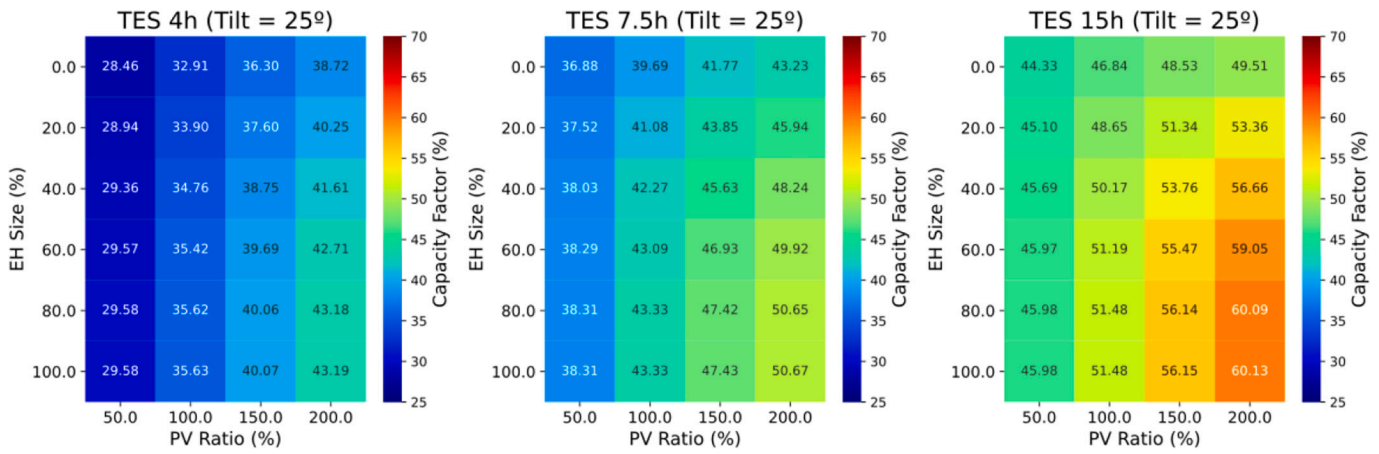

Fig. 16. Capacity Factor for the different hybrid CSP/PV configurations in scenario (d).

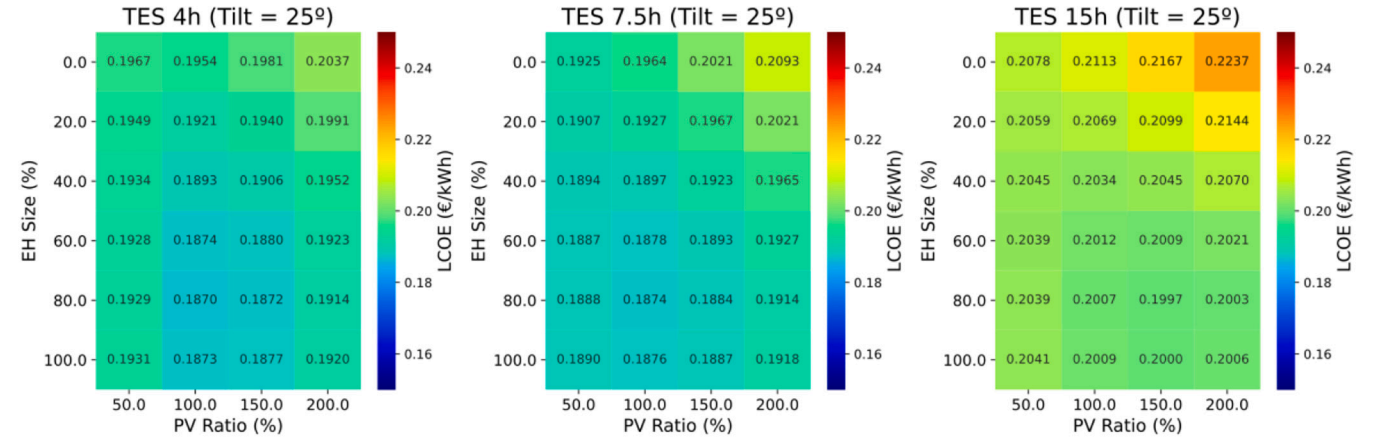

Fig. 17. LCOE for the different hybrid CSP/PV configurations in scenario (d).

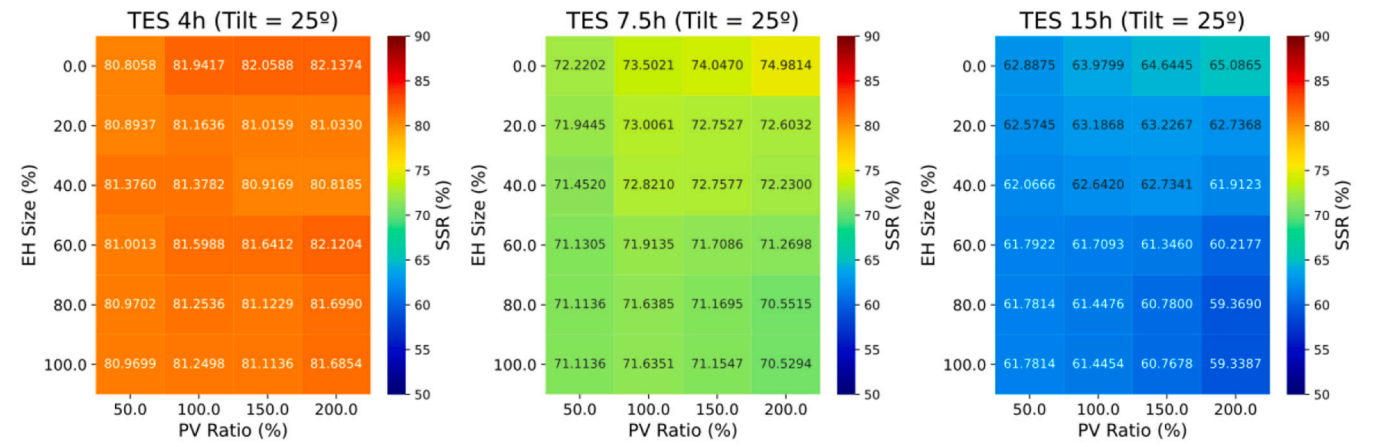

Fig. 18. Self-Supply Ratio for the different hybrid CSP/PV configurations in scenario (d).

trend as in scenario (b) with slightly higher values than the latter due to the effect of the use of an electrical heater.

The inclusion of an electrical heater in the system alters the optimal configuration that minimizes the LCOE for the three analyzed plants, as we can see in Fig. 17. Table 7 presents the optimal configurations for LCOE for the three plant configurations analyzed.

The addition of an electrical heater of the same power (80% of the PV field) results in a small reduction of the LCOE for all the TES capacities analyzed with respect to scenario (b) and an increase of the optimal PV ratio, except for TES 4 h. The optimal PV ratio increases more in plants with larger TES sizes (0% to TES 4 h, 25% to TES 7.5 h and 66.6% to TES 15 h). This is because the PV field's excess energy can be efficiently used by the electrical heater in this design because it has a bigger thermal storage capacity, enabling larger PV plant sizes. When we calculate the ratio between the surplus PV energy from the field and the energy consumed by the electrical heaters, the configuration with a 4-h storage

Table 7
LCOE optimal configurations for three hybrid CSP/PV plants analyzed in scenario (d).

CSP plant	Scenario (b)				Scenario (d)				
	PV Ratio (%)	Tilt (°)	LCOE (€/kWh)	CF (%)	PV Ratio (%)	Tilt (°)	LCOE (€/kWh)	CF (%)	Electrical Heater Size (%)
TES 4 h	130	25	0.1910	35.77	130	25	0.1866	38.44	80
TES 7.5 h	80	25	0.1874	39.77	100	25	0.1873	43.33	80
TES 15 h	90	25	0.2038	47.73	150	25	0.1997	56.13	80

capacity has a value of 82%, the 7.5-h TES configuration has a value of 84%, and the 15-h TES configuration has a value of 93%. This proves how larger TES size combinations make better use of excess PV energy.

With respect to SSR in this scenario, the behavior differs, as we can see in Fig. 18. It is observed that as the size of the electrical heater increases, increasing the PV ratio reduces the SSR. This is because the use of the electrical heater increases the thermal energy stored in the tanks, thereby increasing the CSP plant's production and consequently, its level of parasitic consumption, with the most significant increase occurring in nighttime self-consumption that the PV plant cannot cover.

4.3. PV only for CSP self-consumption. Scenario (c)

For this scenario (c), Fig. 19 shows that in the three analyzed configurations, the CF does not increase for PV ratio greater than 20%. This is attributed to the inability to inject PV-generated energy into the grid in this scenario. Consequently, increasing the size of the PV field does not lead to an increase in electricity production beyond the savings achieved by the CSP plant due to reduced parasitic.

Regarding the LCOE, as shown in the Fig. 20, a minimum value has been reached for a PV ratio of 20% and a tilt of 15° in all the cases analyzed, followed by a sharp increase. This is because with low inclinations of PV panels, we obtain more production in the summer months and less in the winter months compared to the inclination of the panels that maximizes annual PV production, which in the case of Seville is 25°. In this scenario, where PV energy cannot be used to inject into the grid but only to cover self-consumption, the optimal configuration is the one that maximizes the utilization of energy to cover the plant's CSP self-consumption throughout the year. This optimal configuration is found at tilts lower than the one that maximizes annual PV production. To better understand this concept, we simulate a single day in the summer period and a single day in the winter period for TES 7.5 h, PV ratio 20% and tilt 15° and 25°.

Annually, the PV plant with a tilt of 25° produces 20.36 GWh, of which 13.64 GWh are used to satisfy CSP self-consumption, while the plant with a tilt of 15° produces 20.07 GWh and utilizes 13.69 GWh. In Fig. 21, which represents the power of CSP self-consumption, PV production for both tilts, and the PV power used to cover CSP self-consumption for both tilts, it is observed that for a summer day, a tilt of 15° is capable of covering a higher percentage of self-consumption, whereas on a winter day, the effect is the opposite, as seen in Fig. 22. Annually, this difference leans towards a lower tilt than the optimum, as already discussed with the annual data of the plant.

Regarding the SSR, a behavior analogous to previous cases is observed in Fig. 23, with higher values being evident for low inclinations of PV panels.

4.4. Economic sensitivity analysis

To evaluate how these cost changes affect the economic viability of the hybrid plant, we have focused on one of the possible operational scenarios, scenario (c). This analysis allows us to extrapolate the trend of the results to other operational scenarios based on the size of the PV plant introduced, thereby influencing the reduction of LCOE. By focusing on scenario (c), we can evaluate how different price scenarios affect the hybrid plant's ability to reduce costs and improve efficiency without relying on the ability to inject energy into the grid, using it solely to cover the self-consumption of the CSP plant. Fig. 24, Fig. 25 and Fig. 26 show the evolution of LCOE for different scenarios varying the PV ratio for a PV panel tilt of 25°.

All scenarios show improvements in LCOE for all configurations analyzed, with these improvements being more pronounced in the Advanced scenario where PV costs are lower. It can be observed that for the lowest cost scenario (Advanced 2050), as we increase the TES (thermal energy storage), increasing the PV ratio from the optimum reached in the original scenario (20%), the increase in LCOE becomes less pronounced, shifting the optimum to 15 h TES, changing from 20% to 30%. This is due to the low costs and the fact that the level of self-consumption is higher in the plant with larger TES capacity, thereby increasing the PV energy allocated to this purpose.

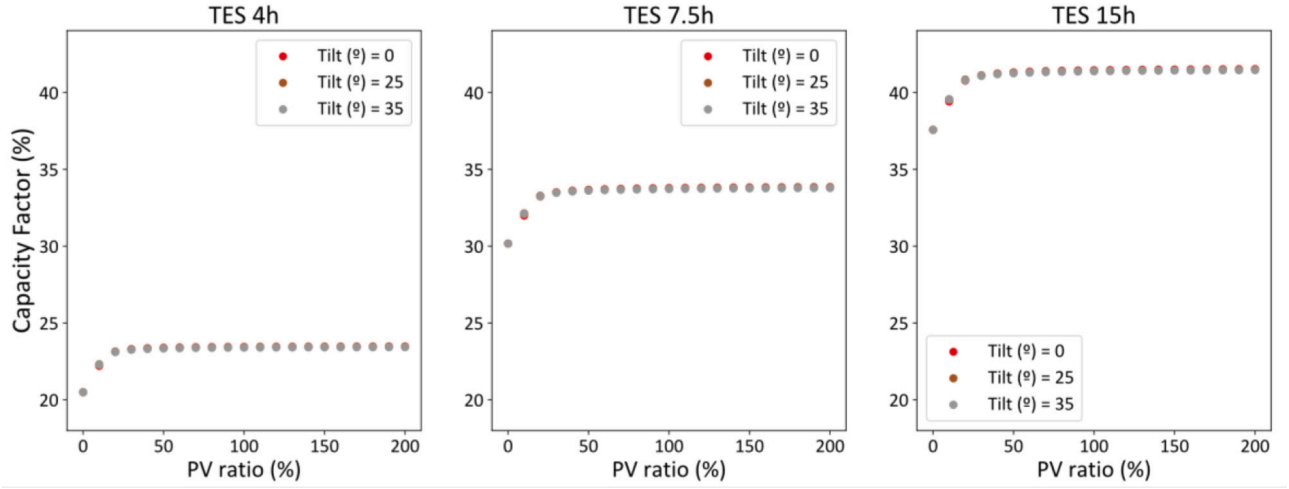

Fig. 19. Capacity Factor for the different hybrid CSP/PV configurations in scenario (c).

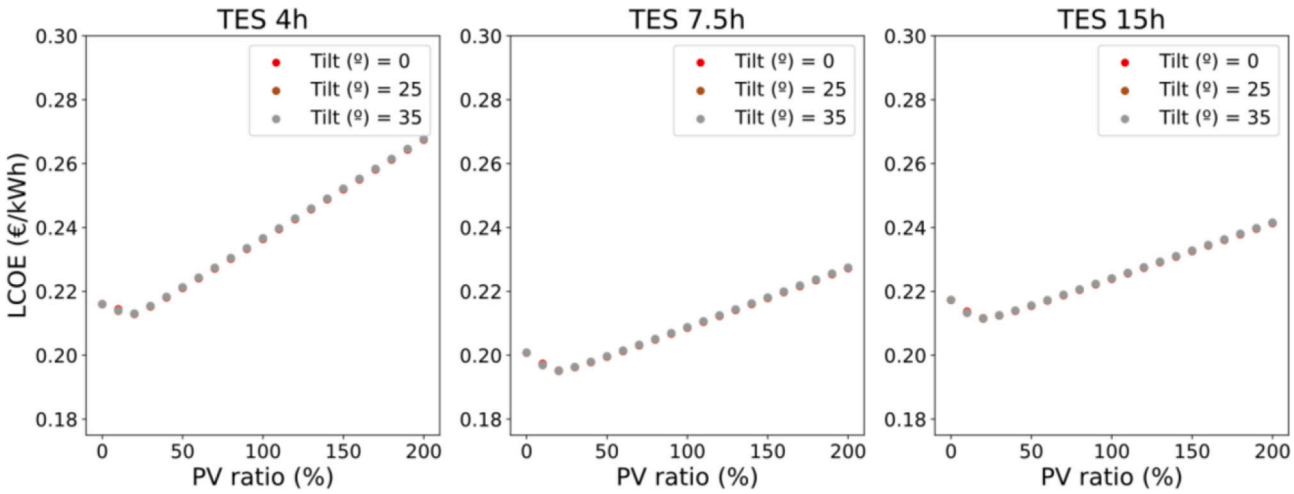

Fig. 20. LCOE for the different hybrid CSP/PV configurations in scenario (c).

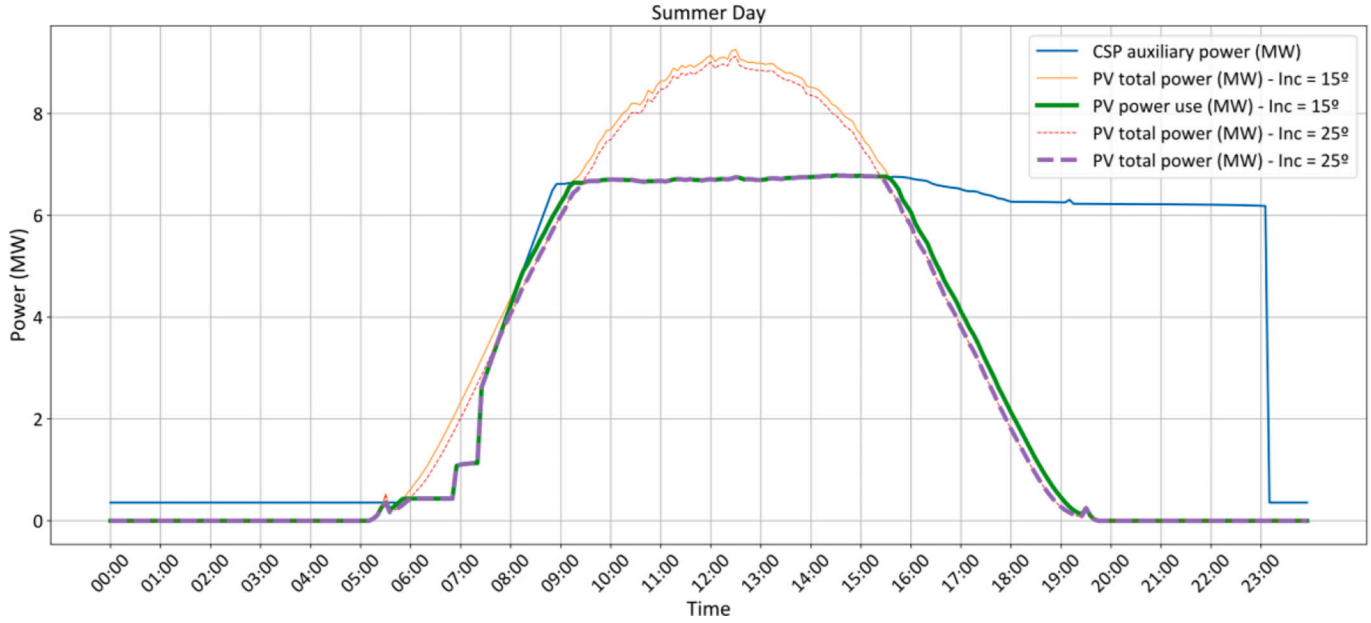

Fig. 21. CSP auxiliary consumption from a summer day to TES 7.5 h and PV ratio 20%.

5. Summary and conclusions

This study presents the development of a simulation tool using Modelica and OpenModelica to analyze and optimize the performance of CSP/PV hybrid plants and its application to the analysis of retrofitting CSP plants with a PV field for different cases and scenarios. The results offer valuable insights into the interplay between different configurations of CSP and PV plants and the influence of key variables, such as PV ratio and TES size, on the hybrid plant's overall performance.

In scenario (a), increasing the PV ratio leads to reductions in both CF and LCOE due to the ability to export energy from the PV field, which has a lower cost compared to CSP. Regarding the SSR, the presence of smaller TES allows for higher SSR values due to the reduced nighttime production from the CSP field, concentrating production during daylight hours when the PV field can meet the self-consumption needs of the CSP field. For PV ratio values greater than 50%, the SSR tends to stabilize.

In scenario (b), the LCOE reaches its minimum at a specific PV ratio (130% for 4 h TES and PV tilt 25°, 80% for 7.5 h TES and PV tilt 25° and 90% for 15 h TES and PV tilt 25°). This is because, as we increase the TES, the CSP plant's ability to export to the grid becomes greater, reducing the PV plant's export capacity, thus reaching optimum configurations at smaller sizes. The introduction of an electrical heater reduces the LCOE by increasing the TES capacity through the utilization of PV energy that could not be exported to the grid, thereby increasing the CF. The impact of the electrical heater becomes more significant as the TES size increases, allowing a greater amount of energy to be directed from the PV field to the electrical heater. For a TES 4 h, the optimal PV ratio does not change; for a TES 7.5 h, it increases by 25%; and for a TES 15 h, it increases by 66.66%.

In scenario (c), we observe that the LCOE reaches its minimum value for a PV ratio of 20% and a PV tilt 20°. The reduction in the tilt of the PV panels in this configuration compared to the one that maximizes annual production, where only PV energy is used to meet CSP self-consumption, is because during summer days, a lower tilt than the one maximizing annual production can satisfy higher CSP self-consumption, with the opposite occurring on winter days. By computing annually, more CSP self-consumption can be satisfied with a lower tilt than the optimal for annual production. The cost sensitivity analysis reveals that a reduction in PV plant costs can yield more favorable techno-economic outcomes, potentially altering the optimal economic configurations. This

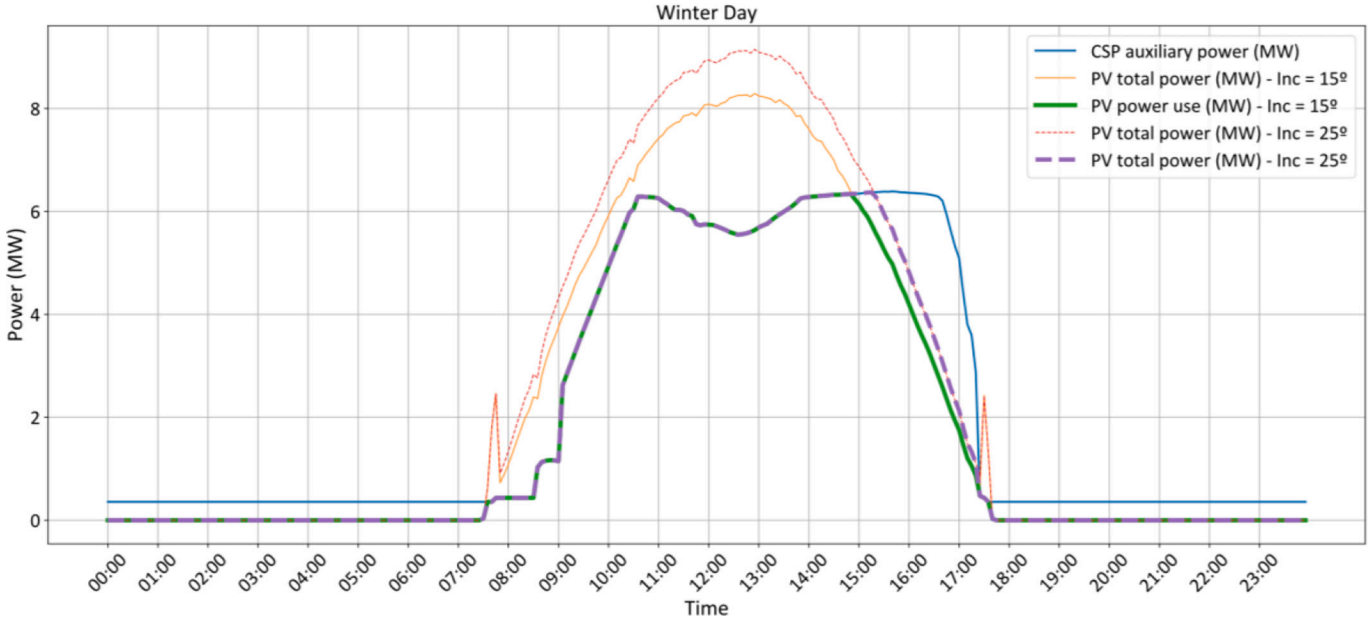

Fig. 22. CSP auxiliary consumption from a winter day to TES 7.5 h and PV ratio 20%.

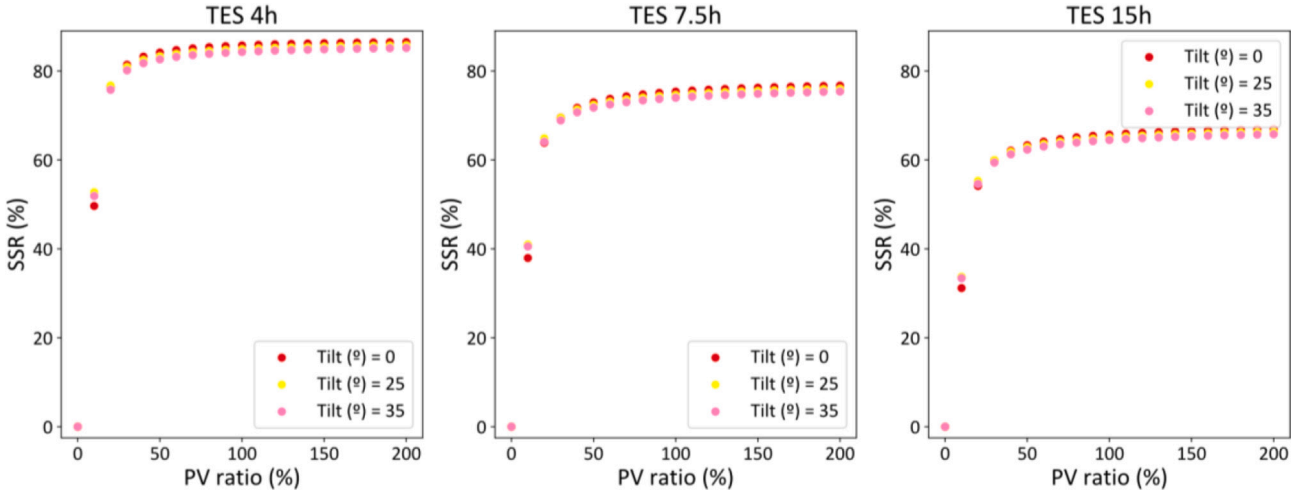

Fig. 23. SelfSupply Ratio for the different hybrid CSP/PV configurations in scenario (c).

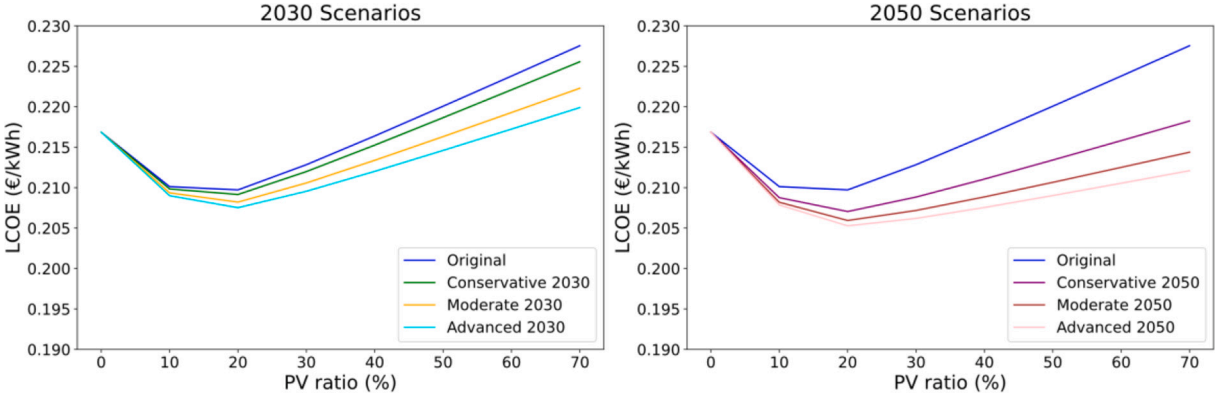

Fig. 24. Economic scenarios for 4 h TES.

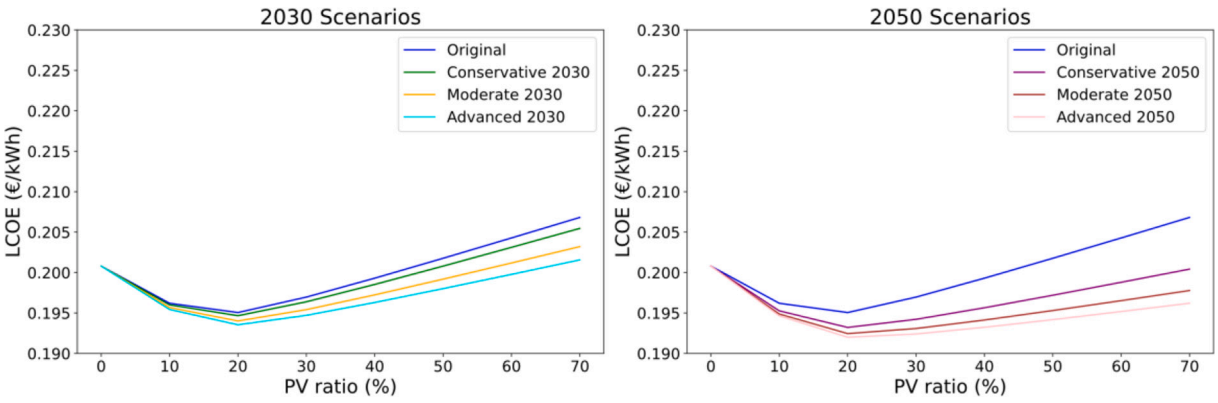

Fig. 25. Economic scenarios for 7.5 h TES.

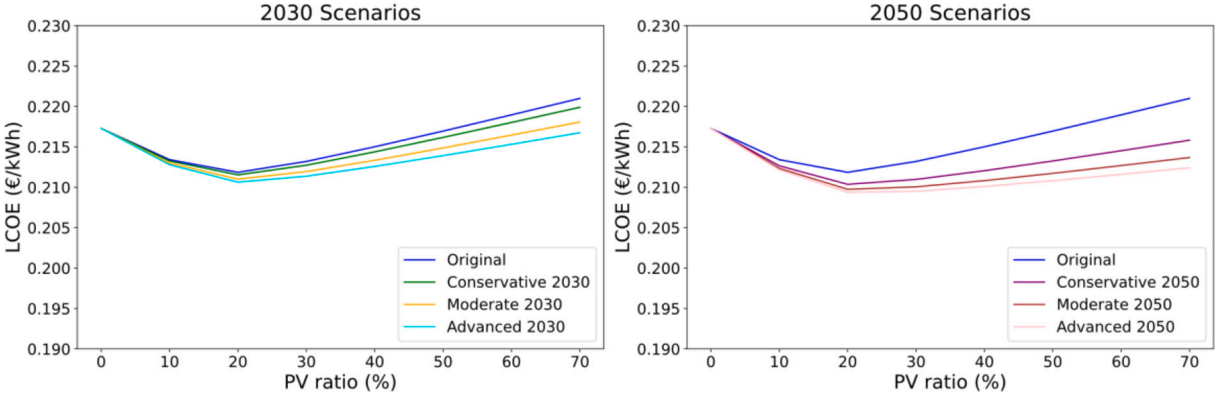

Fig. 26. Economic scenarios for 15 h TES.

underscores the significant sensitivity of these studies to equipment costs.

In conclusion, retrofitting CSP plants with photovoltaic systems to cover self-consumption is a feasible and effective approach to reduce the LCOE compared to standalone CSP plants, provided a proper balance between the size of the photovoltaic plant and the thermal storage capacity is achieved. This enhances the competitiveness of such plants. Hybridizing CSP/PV has the advantage of utilizing the same resource for both plants, making the results obtained from retrofitting CSP plants with PV in this location applicable to other sites with existing CSP plants and high solar resources. The use of simulation tools, such as the one developed in this study, allows for the exploration of different configurations and scenarios to optimize the performance and economic viability of hybrid CSP/PV plants based on the specific conditions of each location.

CRediT authorship contribution statement

José A. López-Álvarez: Writing – original draft, Validation, Software, Methodology, Investigation, Formal analysis, Data curation, Conceptualization. **Miguel Larrañeta:** Writing – review & editing, Supervision, Methodology, Investigation, Conceptualization. **Isidoro Lillo-Bravo:** Visualization, Validation, Supervision, Data curation. **Manuel A. Silva-Pérez:** Writing – review & editing, Validation, Methodology, Conceptualization.

Declaration of competing interest

The authors declare that they have no known competing financial interests or personal relationships that could have appeared to influence the work reported in this paper.

Data availability

Data will be made available on request.

Acknowledgments

This work was supported by Grant RYC2021-032300-I, funded by the Spain Ministry of Science and Innovation/State Research Agency/10.13039/501100011033 and by the European Union "NextGenerationEU/Recovery, Transformation and Resilience Plan".

This work has been carried out in the frame of the project "Exploitation of the synergies of thermosolar and photovoltaic technologies for the development of solar hybrid systems of electricity production (ASDELSOL)" funded by the Junta de Andalucía (Spain) in the frame of the Andalusian investigation development and innovation plan (PAIDI 2020).

Declaration of generative AI and AI-assisted technologies in the writing process

During the preparation of this work the author(s) used ChatGPT to improve the quality of the grammar and redaction. After using this tool/service, the author(s) reviewed and edited the content as needed and take(s) full responsibility for the content of the publication.

References

[1] International Energy Agency, International Energy Agency (IEA) World Energy Outlook 2022," Https://Www.Iea.Org/Reports/World-Energy-Outlook-2022/Executive-Summary, p. 524, 2022, [Online]. Available: https://www.iea.org/reports/world-energy-outlook-2022.

[2] IRENA. Renewable capacity statistics 2023. Abu Dhabi: International Renewable Energy Agency; 2023.
[3] IRENA. Renewable power generation costs in 2022. Abu Dhabi: International Renewable Energy Agency; 2023.
[4] Zurita A, et al. Techno-economic evaluation of a hybrid CSP + PV plant integrated with thermal energy storage and a large-scale battery energy storage system for base generation. Sol Energy 2018;173(January):1262–77. https://doi.org/10.1016/j.solener.2018.08.061.
[5] Parrado C, Girard A, Simon F, Fuentealba E. 2050 LCOE (Levelized cost of energy) projection for a hybrid PV (photovoltaic)-CSP (concentrated solar power) plant in the Atacama Desert, Chile. Energy 2016;94:422–30. https://doi.org/10.1016/j.energy.2015.11.015.
[6] Starke AR, Cardemil JM, Escobar R, Colle S. Multi-objective optimization of hybrid CSP+PV system using genetic algorithm. Energy 2018;147:490–503. https://doi.org/10.1016/j.energy.2017.12.116.
[7] Hassani SE, Ouali HAL, Moussaoui MA, Mezrhab A. Techno-economic analysis of a hybrid CSP/PV plants in the eastern region of Morocco. Appl Sol Energy (English Transl Geliotekhnika) 2021;57(4):297–309. https://doi.org/10.3103/S0003701X21040046.
[8] Starke AR, Cardemil JM, Escobar RA, Colle S. Assessing the performance of hybrid CSP + PV plants in northern Chile. Sol Energy 2016;138:88–97. https://doi.org/10.1016/j.solener.2016.09.006.
[9] Green A, Diep C, Dunn R, Dent J. High capacity factor CSP-PV hybrid systems. Energy Procedia 2015;69:2049–59. https://doi.org/10.1016/j.egypro.2015.03.218.
[10] Zhai R, Chen Y, Liu H, Wu H, Yang Y, Hamdan MO. Optimal design method of a hybrid CSP-PV plant based on genetic algorithm considering the operation strategy. Int J Photoenergy 2018;2018. https://doi.org/10.1155/2018/8380276.
[11] Petrollese M, Cocco D. Optimal design of a hybrid CSP-PV plant for achieving the full dispatchability of solar energy power plants. Sol Energy 2016;137:477–89. https://doi.org/10.1016/j.solener.2016.08.027.
[12] Oyekale J, Heberle F, Petrollese M, Brüggemann D, Cau G. Biomass retrofit for existing solar organic Rankine cycle power plants: conceptual hybridization strategy and techno-economic assessment. Energy Convers Manag 2019;196(June):831–45. https://doi.org/10.1016/j.enconman.2019.06.064.
[13] Otanicar TP, Wingert R, Orosz M, Mcpheeters C. Concentrating photovoltaic retrofit for existing parabolic trough solar collectors : Design, experiments, and levelized cost of electricity. Appl Energy 2020;265(February):114751. https://doi.org/10.1016/j.apenergy.2020.114751.
[14] Goel N, O'Hern H, Orosz M, Otanicar T. Annual simulation of photovoltaic retrofits within existing parabolic trough concentrating solar powerplants. Sol Energy 2020;211(March):600–12. https://doi.org/10.1016/j.solener.2020.09.081.
[15] Felsberger R, Buchroithner A, Gerl B, Schweighofer B, Wegleiter H. Design and testing of concentrated photovoltaic arrays for retrofitting of solar thermal parabolic trough collectors. Appl Energy 2021;300(July):117427. https://doi.org/10.1016/j.apenergy.2021.117427.
[16] Orosz M, Zweibaum N, Lance T, Ruiz M, Morad R. Spectrum-splitting hybrid CSP-CPV solar energy system with standalone and parabolic trough plant retrofit applications. AIP Conf Proc 2016;1734. https://doi.org/10.1063/1.4949170.
[17] Carvajal JL, Barea JM, Barragan J, Ortega C. PV integration into a CSP plant. AIP Conference Proceedings 2017;1850(June):2017. https://doi.org/10.1063/1.4984482.
[18] S.-J. Bode, A. Cuellar, and I. Perez, "Retrofitting operating CSP plants with PV to power auxiliary loads – technical consideration and case study," AIP Conf Proc, vol. 2126, no. 1, p. 90003, Jul. 2019, doi: https://doi.org/10.1063/1.5117605.
[19] Riffelmann KJ, Weinrebe G, Balz M. Hybrid CSP-PV plants with integrated thermal storage. AIP Conf Proc 2022;2445. https://doi.org/10.1063/5.0086610.
[20] Gedle Y, et al. Analysis of an integrated CSP-PV hybrid power plant. AIP Conf Proc 2022;2445(May). https://doi.org/10.1063/5.0086236.
[21] Pilotti L, Colombari M, Castelli AF, Binotti M, Giaconia A, Martelli E. Simultaneous design and operational optimization of hybrid CSP-PV plants. Appl Energy 2022;331(November):120369. 2023, https://doi.org/10.1016/j.apenergy.2022.120369.
[22] Richter P, Trimborn T, Aldenhoff L. Predictive storage strategy for optimal design of hybrid CSP-PV plants with immersion heater. Sol Energy 2021;218:237–50. https://doi.org/10.1016/j.solener.2020.11.005.
[23] The Modelica Association. https://modelica.org/; 2023. accessed Jun. 02.
[24] Fritzson P, et al. The OpenModelica modeling, simulation, and software development environment. Simul News Eur 2005;44:8–16 [Online]. Available: http://www.sne-journal.org/fileadmin/user_upload/tx_pubdb/sne_15_2_3-44_45_webres_01.pdf.
[25] UNE 206011. Solar Thermal Electric Plants. Procedure for Generating a Representative Solar Year. 2014.
[26] Iqbal M. Chapter 11 - SOLAR RADIATION INCIDENT ON TILTED PLANES ON THE EARTH'S SURFACE. In: An Introduction to Solar Radiation. Academic Press; 1983. p. 303–32.
[27] Iqbal M. Chapter 1 - SUN–EARTH ASTRONOMICAL RELATIONSHIPS. In: An introduction to solar radiation. Academic Press; 1983. p. 1–28.
[28] Scott P, Alonso ADLC, Hinkley JT, Pye J. SolarTherm: a flexible Modelica-based simulator for CSP systems. AIP Conf Proc 2019;1850(July):2017. https://doi.org/10.1063/1.4984560.
[29] Protermosolar. https://www.protermosolar.com/proyectos-en-espana/; 2024. accessed Jun. 14.
[30] National Renewable Energy Laboratory., "System Advisor Model version 2023.12.17." Golden, CO., 2024, [Online]. Available: sam.nrel.gov.
[31] López-Alvarez JA, Larraneta M, Silva-Pérez MA, Lillo-Bravo I. Impact of the variation of the receiver glass envelope transmittance as a function of the incidence angle in the performance of a linear Fresnel collector. Renew Energy 2020;150:607–15. https://doi.org/10.1016/j.renene.2020.01.016.
[32] Blanco MJ, Amieva JM, Mancillas A. The Tonatiuh Software Development Project: An Open Source Approach to the Simulation of Solar Concentrating Systems. 2005. p. 157–64. https://doi.org/10.1115/IMECE2005-81859.
[33] Wendelin T, Dobos A, Lewandowski A. SolTrace: a ray-tracing code for complex solar optical systems. Contract 2013;303(October):275–3000.
[34] M. Geyer, E. Lüpfert, R. Osuna, P. Nava, J. Langenkamp, and E. Mandelberg, "EUROTROUGH - Parabolic Trough Collector Developed for Cost Efficient Solar Power Generation," *11th SolarPACES Int Symp Conc Sol Power Chem Energy Technol*, no. October 2015, p. 7, 2002, [Online]. Available: http://sbp.de/es/html/contact/download/EuroTrough_Paper2002.pdf.
[35] King DL, Boyson WE, Kratochvil JA. PHOTOVOLTAIC ARRAY PERFORMANCE MODEL. November. 2003.
[36] Petrollese M, Cocco D. Optimal design of a hybrid CSP-PV plant for achieving the full dispatchability of solar energy power plants. Sol Energy 2016;137:477–89. https://doi.org/10.1016/j.solener.2016.08.027.
[37] National Renewable Energy Laboratory. NREL Concentrating Solar Power Projects. https://solarpaces.nrel.gov/project/andasol-1. [Accessed 15 February 2024].
[38] Wagner MJ, Gilman P. Technical manual for the SAM physical trough model, by National Renewable Energy Laboratory (NREL, U.S. Department of Energy). Natl Renew Energy Lab 2011;303(June):275–3000 [Online]. Available, http://www.nrel.gov/docs/fy11osti/51825.pdf.
[39] Kost C, et al. FRAUNHOFER INSTITUT FOR SOLAR ENERGY SYSTEMS ISE LEVELIZED COST OF ELECTRICITY RENEWABLE ENERGY TECHNOLOGIES Levelized Cost of Electricity Renewable Energy Technologies. November. 2013.
[40] NREL (National Renewable Energy Laboratory). Annual Technology Baseline2022; 2022. https://atb.nrel.gov/ [accessed Jun. 24, 2024].
[41] National Renewable Energy Laboratory., "System Advisor Model Version 2021.12.2 (SAM 2021.12.2)." 2021, [Online]. Available: https://https//sam.nrel.gov.
[42] Giuliano S, Puppe M, Noureldin K. Power-to-heat in CSP systems for capacity expansion. AIP Conf Proc 2019;2126(July):2019. https://doi.org/10.1063/1.5117589.
[43] Zurita A, Mata-Torres C, Cardemil JM, Escobar RA. Assessment of time resolution impact on the modeling of a hybrid CSP-PV plant: A case of study in Chile. Sol Energy 2020;202(April 2019):553–70. https://doi.org/10.1016/j.solener.2020.03.100.